Nature Environment and Pollution Technology
An International Quarterly Peer-Reviewed Open Access Journal

p-ISSN: 0972-6268 | e-ISSN: 2395-2454 Vol. 25 | No. 4 | Article ID B4429 | 2026

RESEARCH ARTICLE https://doi.org/10.46488/NEPT.2026.v25i04.B4429 OPEN ACCESS

Three Decades of Urban Heat Dynamics in Patna, India: A Remote Sensing-Based Hotspot Analysis

Avinash Kumar Singh† and Manoj Kumar
Department of Architecture and Planning, National Institute of Technology, Patna 800005, Bihar, India
†Corresponding author: Avinash Kumar Singh; avinash.singh1603arch@nitp.ac.in

ARTICLE HISTORY

Received: 02-02-2026
Revised: 17-03-2026
Accepted: 08-04-2026

KEYWORDS

Land surface temperature (LST)
Remote sensing
Vegetation dynamics
Urban heat dynamics

CITE THIS ARTICLE

Singh, A.K. and Kumar, M. 2026. Three decades of urban heat dynamics in Patna, India: A remote sensing-based hotspot analysis. *Nature Environment and Pollution Technology*, 25(4), B4429.

COPYRIGHT & LICENCE

© 2026 The Authors
Open Access under CC BY 4.0.

PUBLISHED BY

TECHNOSCIENCE PUBLICATIONS

ABSTRACT

Rapid urbanization in tropical cities has intensified surface thermal stress, yet the long-term persistence and spatial structure of urban heat remain poorly understood, particularly in rapidly expanding cities of the Global South. This study investigates three decades (1995–2025) of urban thermal dynamics in Patna, India, with a focus on identifying long-term temperature trends, examining their relationship with vegetation greenness and built-up expansion, and assessing the spatial persistence of urban heat hotspots. Using a longitudinal remote sensing framework, Land Surface Temperature (LST) was analyzed alongside the Normalized Difference Vegetation Index (NDVI) and Normalized Difference Built-up Index (NDBI), derived from multi-decadal Landsat imagery processed in a cloud-based environment. A comprehensive spatiotemporal analytical approach integrating non-parametric trend analysis, correlation testing, hotspot persistence mapping, and multivariate regression modeling was employed to capture both temporal trajectories and spatial stability of urban warming. Results reveal a statistically significant increase in mean LST at a rate of approximately 0.13°C yr^{-1}, accompanied by a strong and monotonic rise in built-up intensity, while vegetation greenness exhibits high interannual variability without a significant long-term trend. Spatial analysis identifies a marked regime shift around the mid-2000s, after which high-temperature zones persistently dominate more than 95% of the urban area, with no observed reversals over the subsequent two decades. Regression results confirm built-up expansion as the sole statistically significant predictor of long-term surface warming at the city scale. Collectively, the findings suggest that Patna has experienced a sustained shift toward long-term dominance of high-temperature zones, indicating increasing persistence of urban heat across the city. The study provides robust empirical evidence of long-term urban heat persistence in a tropical city and offers a transferable analytical framework for identifying sustained thermal risk to support climate-sensitive urban planning and adaptation strategies.

1. INTRODUCTION

Rapid urbanization, coupled with global climate warming, has intensified surface thermal stress in cities worldwide, making urban heat a critical environmental challenge of the twenty-first century (Halefom et al. 2024, Sachindra et al. 2023). Urban land cover transformation, including increased impervious surfaces, reduced vegetation, and enhanced anthropogenic heat emissions, fundamentally alters surface–atmosphere energy exchanges, leading to elevated Land Surface Temperature (LST) (Mishra & Arya 2024, Nath 2025, Weng et al. 2004). Rising LST amplifies heat exposure, degrades outdoor thermal comfort, increases cooling energy demand, and exacerbates heat-related morbidity and mortality (Gupta & Aithal 2022, Halder et al. 2025a, Spangler et al. 2022). These impacts are particularly severe in tropical cities, where high baseline temperatures, prolonged

heat seasons, and dense populations create conditions of persistent thermal stress (Chow et al. 2016, Priya & Senthil 2024).

Satellite-derived LST provides a robust and spatially explicit indicator for analyzing urban thermal environments at multiple scales (Amindin et al. 2021, Chen 2022). Remote sensing-based studies commonly employ the Normalized Difference Vegetation Index (NDVI) and the Normalized Difference Built-up Index (NDBI) to explain spatial and temporal variations in LST, representing vegetative cooling and impervious surface expansion, respectively (Beck et al. 2006, Guha et al. 2018). Extensive evidence demonstrates a negative relationship between LST and NDVI due to evapotranspirative cooling, and a positive relationship between LST and NDBI associated with heat storage and reduced surface permeability (Ma et al. 2025, Pradeep Kumar et al. 2023). Collectively, these studies and reviews demonstrate that although spatial heterogeneity and spatiotemporal variability of urban LST are well-recognized research themes, methodological limitations and data availability have led many studies to focus on short time spans, selected years, or coarse temporal comparisons rather than continuous long-term analyses (Mahata et al. 2024, Voogt & Oke 2003, Zhou et al. 2014). Such approaches limit the ability to identify long-term structural changes in urban thermal behavior and to distinguish persistent urban warming from short-term climatic variability (Halder et al. 2025b, Rasul et al. 2017). A particularly underexplored aspect is urban heat hotspot persistence, defined as the degree to which high-LST zones remain spatially stable over extended periods (Halder et al. 2026). While urban heat islands are frequently mapped for individual years, few studies systematically assess whether these hotspots are transient or structurally embedded within the urban fabric (Amir Siddique et al. 2023, Heaviside et al. 2017, Qi et al. 2024).

These research gaps are particularly acute in rapidly urbanizing tropical cities of the Global South, where unplanned urban expansion and weak land-use governance exacerbate thermal vulnerability (Grimm et al. 2008, Hsu et al. 2021, Seto et al. 2012). Cities across the Indo-Gangetic Plain exemplify these challenges but remain markedly underrepresented in long-term urban climate analyses (Mohan & Kandya 2015). Among them, Patna, a rapidly expanding tropical city in India, has undergone substantial land-use and land-cover transformation over the past three decades, characterized by accelerated built-up expansion and increasing fragmentation and loss of vegetated surfaces (Mohamed et al. 2025). Despite its climatic vulnerability, Patna has received limited attention in multi-decadal urban thermal studies. Unlike most previous urban heat studies that focus on short-term trends or isolated snapshot years, this research explicitly quantifies the long-term spatial persistence of urban heat hotspots using a continuous 31-year satellite record, providing new insights into structurally embedded thermal risk in a tropical city of the Global South.

In this context, the study aims to conduct a three-decade (1995–2025) spatiotemporal analysis of urban thermal dynamics in Patna, integrating Landsat-derived LST with NDVI and NDBI. The study objectives are to (i) quantify long-term trends in surface temperature, vegetation greenness, and built-up intensity, (ii) examine their statistical relationships at the city scale, and (iii) assess the spatial persistence and dominance of urban heat hotspots. By combining non-parametric trend analysis, correlation assessment, hotspot persistence mapping, and multivariate regression, this research provides a technically robust and transferable framework for identifying structurally persistent urban heat in data-scarce tropical cities, with direct implications for climate-sensitive urban planning and heat mitigation strategies.

2. MATERIALS AND METHODS

2.1. Study Area

The study focuses on Patna Municipal Corporation (PMC), the capital city of the Indian state of Bihar, located in the eastern part of the Indo-Gangetic Plain (IGP) between approximately 25.5°–25.7° N latitude and 85.0°–85.2° E longitude. Patna lies along the southern bank of the Ganga River at an average elevation of about 53 m above mean sea level, making it part of a low-lying alluvial floodplain. The city experiences a tropical wet-and-dry climate (Köppen: Aw), characterized by extremely hot summers (April–June), a monsoon season with high humidity (July–September), and mild winters (December–February). Mean summer air temperatures frequently exceed 40°C, contributing to high baseline thermal stress (CITY OF PATNA 2026) (Fig. 1).

Over the past three decades, Patna has undergone rapid urban expansion driven by population growth, infrastructure development, and economic transformation, resulting in the extensive conversion of agricultural and vegetated land into impervious built-up surfaces (Mishra & Patel 2025). The urban landscape exhibits a heterogeneous spatial structure comprising dense built-up cores, expanding peri-urban zones, fragmented green spaces, and riverine environments (Kumar & Rajak 2023). Although the presence of the Ganga River offers potential cooling effects, these benefits are spatially uneven and increasingly offset by adjacent high-density development (Khan et al. 2021). The city's rapid and largely unplanned urbanization, combined with its climatic setting,

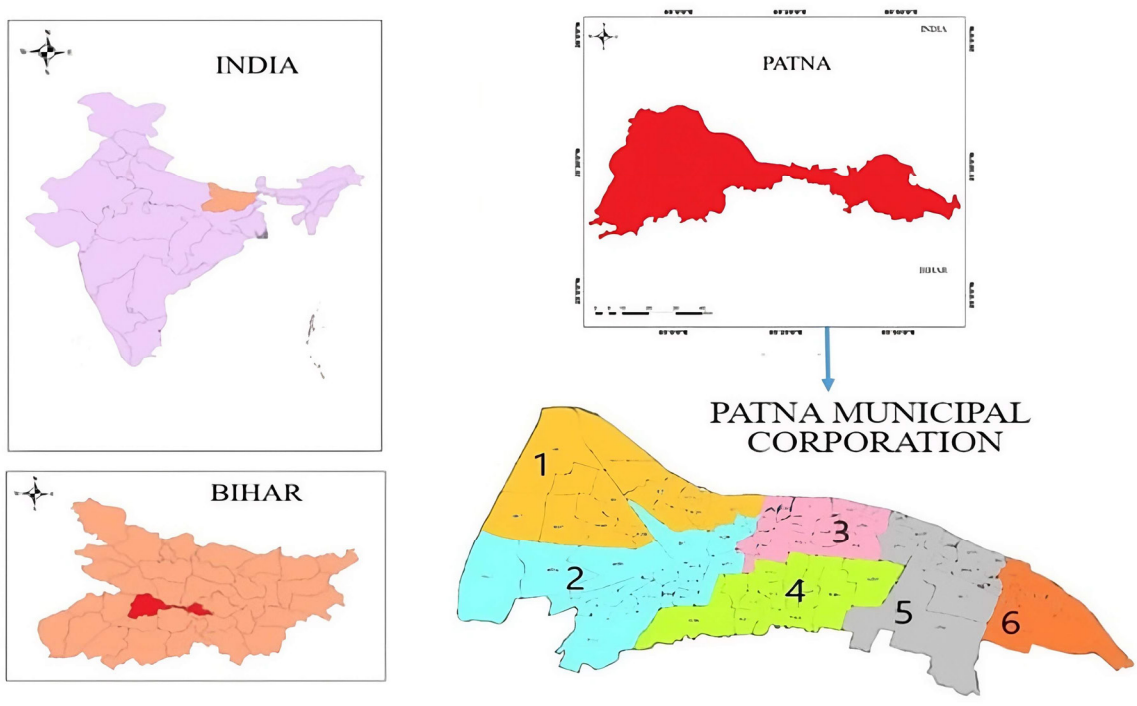


Fig. 1: Study area map with six divisions of PMC.

makes Patna a highly suitable case for examining long-term urban thermal dynamics and the spatial persistence of heat hotspots in tropical megacities (Siddiqui et al. 2022).

2.2. Research Design

This study adopts a quantitative spatiotemporal research design integrating satellite remote sensing, geospatial analysis, and statistical modeling to examine long-term urban thermal dynamics in Patna, India, from 1995 to 2025. The research is grounded in a longitudinal remote sensing framework, enabling the systematic assessment of LST and its relationship with vegetation cover, represented by the NDVI, and built-up expansion, represented by the NDBI. The methodological framework combines non-parametric trend analysis, correlation assessment, spatial hotspot persistence mapping, and multivariate regression modeling to capture both the temporal evolution and spatial persistence of urban heat.

2.3. Datasets

The analysis utilizes multi-decadal satellite imagery acquired from the United States Geological Survey (USGS) and processed using the Google Earth Engine (GEE) cloud computing platform. GEE facilitates the efficient handling of large spatiotemporal datasets while ensuring standardized preprocessing across sensors and years. The Landsat path–row and spatial resolutions of the VNIR and TIR bands across the study period are shown in Table 1.

Landsat imagery from Landsat-5 Thematic Mapper (TM) (1995–2011), Landsat-7 Enhanced Thematic Mapper Plus (ETM+) (1999–2021), and Landsat-8 Operational Land Imager/Thermal Infrared Sensor (OLI/TIRS) (2013–2025) was used. Visible, near-infrared (VNIR), shortwave infrared (SWIR), and thermal infrared (TIR) bands were used to derive NDVI, NDBI, and LST, respectively. All datasets were spatially clipped to the PMC boundary.

Thermal bands, originally available at 100–120 m spatial resolution, depending on sensor specifications, were resampled to 30 m resolution using bilinear interpolation to maintain spatial uniformity across all variables. For each year, annual mean composites were generated using all available cloud-free observations. Cloud and cloud-shadow contamination were minimized using the Fmask algorithm implemented within the GEE environment. This approach

Table 1: Landsat path–row and spatial resolution of VNIR and TIR bands across the study period.

Year	Path-row	Band resolution – VNIR [m]	Band resolution – TIR [m]
1995–2005	141/42	30	120
2005–2015	141/42	30	100, 120
2015–2025	141/42	30	100

ensured temporal consistency and reduced noise arising from atmospheric variability.

2.4. Data Collection Methods

2.4.1. Preprocessing and Index Computation

All imagery underwent standardized preprocessing procedures to ensure radiometric and geometric consistency. Radiometric calibration and conversion to Top-of-Atmosphere (TOA) reflectance were conducted using sensor-specific metadata. Cloud and shadow masking was applied prior to compositing. All raster datasets were co-registered and resampled to a common spatial grid to ensure spectral comparability across sensors and years.

NDVI was calculated using near-infrared (NIR) and red bands following the standard formulation:

$$NDVI = \frac{NIR - Red}{NIR + Red}$$

NDVI values range from −1 to +1, with higher values indicating denser vegetation and greater cooling potential through evapotranspiration.

NDBI was computed using shortwave infrared (SWIR) and near-infrared (NIR) bands as:

$$NDBI = \frac{SWIR - NIR}{SWIR + NIR}$$

Positive NDBI values indicate built-up or impervious surfaces, while negative values represent vegetated or water-covered areas.

Thermal bands were first converted from digital numbers (DN) to spectral radiance:

$$L_\lambda = M_L \times DN + A_L$$

Where M_L and A_L are sensor-specific radiance multiplicative and additive scaling factors.

Radiance was then converted to at-sensor brightness temperature:

$$T_B = \frac{K_2}{\ln\left(\frac{K_1}{L_\lambda}+1\right)}$$

Where K_1 and K_2 are calibration constants.

Land surface emissivity (ε) was estimated using an NDVI-based approach:

$$\varepsilon = 0.004 \times P_v + 0.986$$

Where P_v is the proportion of vegetation calculated as:

$$P_v = \left(\frac{NDVI - NDVI_{min}}{NDVI_{max} - NDVI_{min}}\right)^2$$

Final LST was computed as:

$$LST = \frac{T_B}{1 + \left(\frac{\lambda T_B}{\rho}\right)\ln(\varepsilon)} - 273.15$$

Where l is the wavelength of emitted radiance and $\rho = \frac{hc}{\sigma}$.

2.4.2. Trend Analysis

Long-term trends in LST, NDVI, and NDBI were evaluated using the Mann–Kendall (MK) test, a non-parametric method suitable for environmental time series with non-normal distributions. For a time series $x_1, x_2, \ldots, x_n$, the MK statistic is defined as:

$$S = \sum_{i=1}^{n-1} \sum_{j=i+1}^{n} \text{sgn}(x_j - x_i)$$

where:

$$\text{sgn}(x_j - x_i) = \begin{cases} +1, & x_j - x_i > 0 \\ 0, & x_j - x_i = 0 \\ -1, & x_j - x_i < 0 \end{cases}$$

The variance of S is:

$$Var(S) = \frac{n(n-1)(2n+5) - \sum t(t-1)(2t+5)}{18}$$

The standardized test statistic Z is:

$$Z = \begin{cases} \frac{S-1}{\sqrt{Var(S)}}, & S > 0 \\ 0, & S = 0 \\ \frac{S+1}{\sqrt{Var(S)}}, & S < 0 \end{cases}$$

Trend magnitude was estimated using Sen's slope (β):

$$\beta = \text{Median}\left(\frac{x_j - x_i}{j - i}\right), \forall i < j$$

This estimator provides a robust measure of the annual rate of change for each variable.

2.4.3. Correlation Analysis

The relationships between LST and the surface indices (NDVI and NDBI) were assessed using both Pearson's correlation coefficient (r) and Spearman's rank correlation coefficient (ρ). Linear relationships were evaluated using Pearson's correlation coefficient (r):

$$r = \frac{\sum_{i=1}^{n}(x_i - \bar{x})(y_i - \bar{y})}{\sqrt{\sum_{i=1}^{n}(x_i - \bar{x})^2 \sum_{i=1}^{n}(y_i - \bar{y})^2}}$$

Monotonic relationships and nonlinear relationships were assessed using Spearman's rank correlation coefficient (ρ):

$$\rho = 1 - \frac{6\sum d_i^2}{n(n^2 - 1)}$$

Where d_i is the difference between ranks of paired observations.

Both coefficients were evaluated at a 95% confidence level, ensuring robustness of inferred interactions between surface temperature, vegetation, and built-up intensity.

2.4.4. Hotspot Persistence Analysis

Systematic identification of structurally persistent heat zones was conducted by classifying LST maps for 1995, 2005, 2015, and 2025 into five equal-interval categories ranging from very low to very high temperature. Pixels falling within the high and very high categories were designated as thermal hotspots. A Hotspot Persistence Index (HPI) was computed for each pixel as:

$$HPI_p = \frac{\sum_{t=1}^{T} H_{p,t}}{T}$$

where $H_{p,t} = 1$ if pixel p is classified as a hotspot at time t, and 0 otherwise, with $T = 4$. HPI values range from 0 (no persistence) to 1 (persistent hotspot across all decades). Spatial patterns of hotspot persistence were analyzed and visualized to assess the stability and expansion of heat-stressed zones.

To evaluate the long-term spatial persistence of thermal hotspots, four benchmark years (1995, 2005, 2015, and 2025) were selected from the 31-year dataset. These years represent approximately decadal intervals and were chosen to capture major phases of urban development while reducing the influence of short-term climatic variability and interannual noise commonly present in annual LST observations. While annual LST data were used for temporal statistical analyses, including the Mann–Kendall trend test and Sen's slope estimation, the benchmark-year approach enables a clearer identification of structural spatial transitions in the urban thermal regime. This approach has been widely applied in long-term remote sensing studies to highlight persistent spatial patterns while maintaining the interpretability of multi-decadal changes.

2.4.5. Multiple Regression Analysis

To quantify the relative contributions of vegetation loss and built-up expansion to long-term LST variation, a multiple linear regression model was developed with mean LST as the dependent variable and NDVI and NDBI as the independent variables. The formula is:

$$LST = \alpha + \beta_1(NDVI) + \beta_2(NDBI) + \varepsilon$$

where β_1 and β_2 represent regression coefficients and is the error term.

Model diagnostics were conducted to ensure statistical validity. Regression coefficients were interpreted to assess the dominant drivers of urban thermal increase.

2.5. Software and Analytical Tools

All large-scale geospatial data processing and time-series extraction were conducted using GEE, which enabled efficient handling of multi-decadal satellite datasets within a cloud-computing environment. Statistical analyses and trend assessments were performed using Python, employing the pandas, NumPy, SciPy, and statsmodels libraries, complemented by additional statistical validation in R. Spatial analysis, visualization, and final map production were carried out in QGIS, ensuring accurate spatial representation and cartographic consistency.

3. RESULTS

3.1. Descriptive Temporal Characteristics of LST, NDVI, and NDBI (1995–2025)

The annual mean LST, NDBI, and NDVI time series for Patna from 1995 to 2025 exhibit distinct temporal behaviors (Fig. 2). Mean LST values show substantial interannual variability but an overall upward trajectory across the study period. Mean LST increased from 34.45°C in 1995 to 38.89°C in 2025, with multiple peak years exceeding 42°C. The temporal range of mean LST across the dataset spans approximately 11.3°C, indicating pronounced variability superimposed on a long-term increase.

Mean NDBI values display a near-monotonic rise over time, increasing from 0.0076 in 1995 to 0.1947 in 2025. Unlike LST, NDBI exhibits limited interannual fluctuation and demonstrates a persistent upward trend throughout the

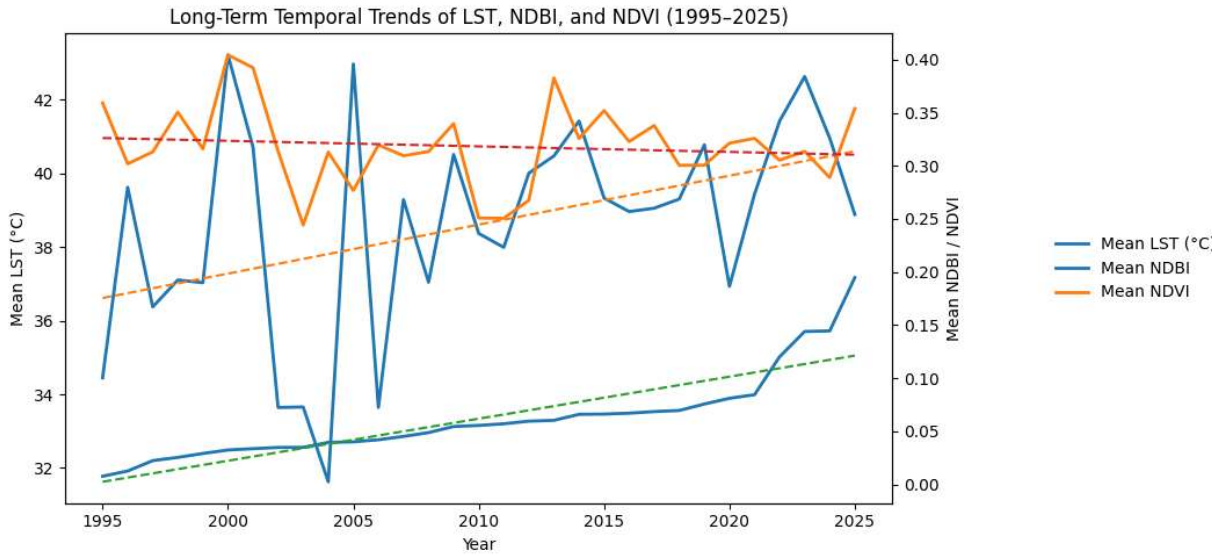


Fig. 2: Long-term temporal trends of LST, NDBI, and NDVI (1995–2025).

Table 2: Modified Mann–Kendall (MMK) trend test and Sen's slope estimator for the period 1995–2025.

Variable	MK Z-value	Trend Direction	p-value	Sen's Slope	95% CI of Sen's Slope	Significant at α = 0.05
Mean LST (°C)	+2.14	Increasing	0.032	+0.1308°C yr⁻¹	+0.018–+0.244 °C yr⁻¹	Yes
Mean NDBI (–)	+7.89	Increasing	<0.001	+0.00269 yr⁻¹	+0.0020–+0.0034 yr⁻¹	Yes
Mean NDVI (–)	−0.41	Decreasing	0.681	−0.00035 yr⁻¹	−0.0021–+0.0014 yr⁻¹	No

observation period. Accelerated increases are evident after approximately 2005, followed by continued growth through the 2010s and early 2020s.

In contrast, mean NDVI values exhibit pronounced interannual fluctuations without a clear monotonic pattern. NDVI values range between 0.24 and 0.40, with episodic peaks and troughs occurring throughout the period. No sustained long-term increase or decrease is visually evident at the city-averaged scale.

3.2. Trend Analysis of LST, NDVI, and NDBI (1995–2025)

The Modified Mann–Kendall (MMK) trend test and Sen's slope estimator for the period 1995–2025 are summarized in Table 2. Mean LST exhibits a statistically significant positive trend, with an MMK Z-value of +2.14 ($p = 0.032$). Sen's slope indicates an annual increase of +0.1308°C yr⁻¹, corresponding to a net increase of approximately +4.05°C over the 31 years. The 95% confidence interval of Sen's slope ranges from +0.018 to +0.244°C yr⁻¹, confirming a consistent upward trend.

Mean NDBI demonstrates a highly significant increasing trend, with an MMK Z-value of +7.89 ($p < 0.001$). Sen's slope for NDBI is +0.00269 yr⁻¹, yielding a cumulative increase of approximately +0.083 between 1995 and 2025. The narrow 95% confidence interval (+0.0020 to +0.0034 yr⁻¹) indicates strong monotonic behavior and minimal uncertainty.

Mean NDVI shows a negative but statistically insignificant trend ($Z = -0.41$, $p = 0.681$). Sen's slope for NDVI is −0.00035 yr⁻¹, with a 95% confidence interval spanning −0.0021 to +0.0014 yr⁻¹ and crossing zero. This result indicates the absence of a detectable monotonic trend in vegetation greenness at the city scale.

3.3. Evolution of LST Class Areas and Thermal Regime Transitions

The temporal evolution of LST class areas from 1995 to 2025 is illustrated in Fig. 3. High-LST zones (Class 4) are present in all 31 years of the study period, indicating uninterrupted dominance. Prior to 2005, the area of Class 4 exhibits expansion and consolidation, while lower-temperature classes (Classes 1–3) remain intermittently present.

From 2005 onward, Class 4 consistently occupies more than 95% of the total urban area, with area values exceeding 103 km² in 21 out of 31 years. Post-2005 variability in Class 4 area is minimal, with a coefficient of variation below 2%, indicating high spatial stability.

Class 1 (lowest LST) areas occur sporadically until 2010. Class 2 areas become increasingly fragmented and occupy less than 0.1% of the total urban area after 2015. Class 3 (moderate LST) persists throughout the study period but shows a systematic reduction, with progressive absorption into Class 4 over time. No year exhibits a re-expansion of lower-LST classes once their areas decline.

A clear shift in the thermal structure is evident between 2004 and 2005, marked by the rapid decline of lower-temperature classes and the sustained dominance of high-LST zones thereafter. After this transition, no reversal to lower thermal classes is observed.

3.4. Spatial Patterns of LST, NDVI and NDBI

The spatial distribution maps of LST, NDVI, and NDBI for the benchmark years 1995, 2005, 2015, and 2025 are shown in Figs. 4–6, revealing pronounced and progressive spatial reorganization of Patna's urban thermal and land-cover structure.

In 1995, the LST map exhibits a heterogeneous thermal landscape characterized by a mosaic of moderate- and high-temperature zones interspersed with clearly identifiable cooler pockets. Lower LST values are spatially concentrated along river-adjacent areas, peripheral zones, and locations with relatively higher vegetation presence, while elevated temperatures appear fragmented and largely confined to the central urban core. The thermal contrast between built-up and non-built-up areas is evident, indicating an early-stage urban heat pattern with incomplete spatial consolidation. By 2005, high-LST zones expand both in extent and continuity. Red and orange regions become more spatially connected, particularly across the central and eastern parts of the city. Cooler zones shrink in size and begin to fragment, losing their earlier spatial coherence. The transition between moderate- and high-temperature areas becomes sharper, suggesting increasing surface heat accumulation and reduced buffering capacity. This period marks a visible shift from a patchy thermal configuration to a more organized and dominant high-temperature structure.

In 2015, the LST surface shows further intensification and spatial homogenization. High-temperature zones dominate most of the urban area, with only scattered, isolated cool patches remaining. These residual cooler zones are small, spatially discontinuous, and largely restricted to specific pockets rather than forming continuous corridors. The contrast between core and peripheral areas diminishes, indicating that elevated surface temperatures are no longer confined to the urban center but have propagated across the broader city extent.

By 2025, the LST map reflects near-complete dominance of high-temperature conditions across Patna. Cooler areas are minimal and highly fragmented, appearing as isolated pixels or small clusters embedded within an otherwise continuous high-LST matrix. The spatial pattern suggests strong thermal uniformity at high temperature levels, with limited spatial variability. This configuration indicates that surface warming has transitioned from localized intensification to a citywide thermal state.

NDVI maps show a contrasting but complementary evolution. In 1995, vegetation greenness is spatially heterogeneous, with relatively large and continuous green patches visible along certain corridors, peripheral zones, and open areas. These patches form discernible clusters that correspond spatially with lower-LST zones, indicating a localized influence of vegetation on surface conditions. By 2005, NDVI patterns become increasingly fragmented. While

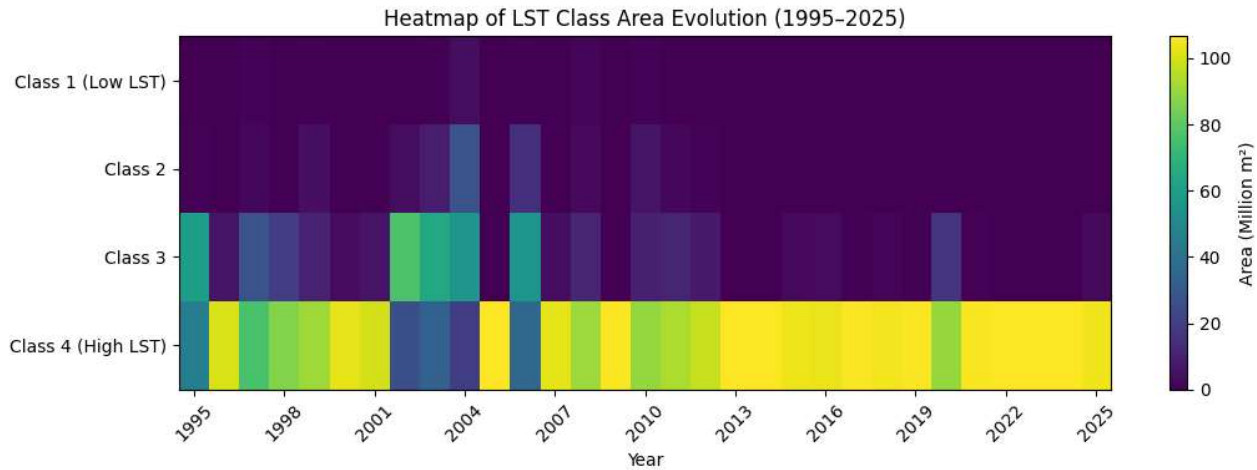


Fig. 3: Temporal evolution of LST class areas from 1995–2025.

vegetation remains present across the city, green patches lose continuity and become interspersed with expanding non-vegetated surfaces. High-NDVI zones are reduced in size and begin to appear as scattered clusters rather than cohesive units. This fragmentation coincides spatially with the expansion of high-LST areas.

In 2015, vegetation greenness persists but exhibits pronounced spatial redistribution. NDVI values remain moderate in selected areas, particularly along certain linear features and peripheral zones; however, these areas are spatially isolated and embedded within predominantly low-NDVI surroundings. The lack of continuous green corridors is evident, indicating reduced spatial effectiveness of vegetation cover.

By 2025, NDVI maps display a highly fragmented greenness pattern. Vegetation patches remain detectable but are small, dispersed, and spatially disconnected. No large or continuous green zones are visible, and low-NDVI surfaces largely surround vegetated areas. This configuration suggests

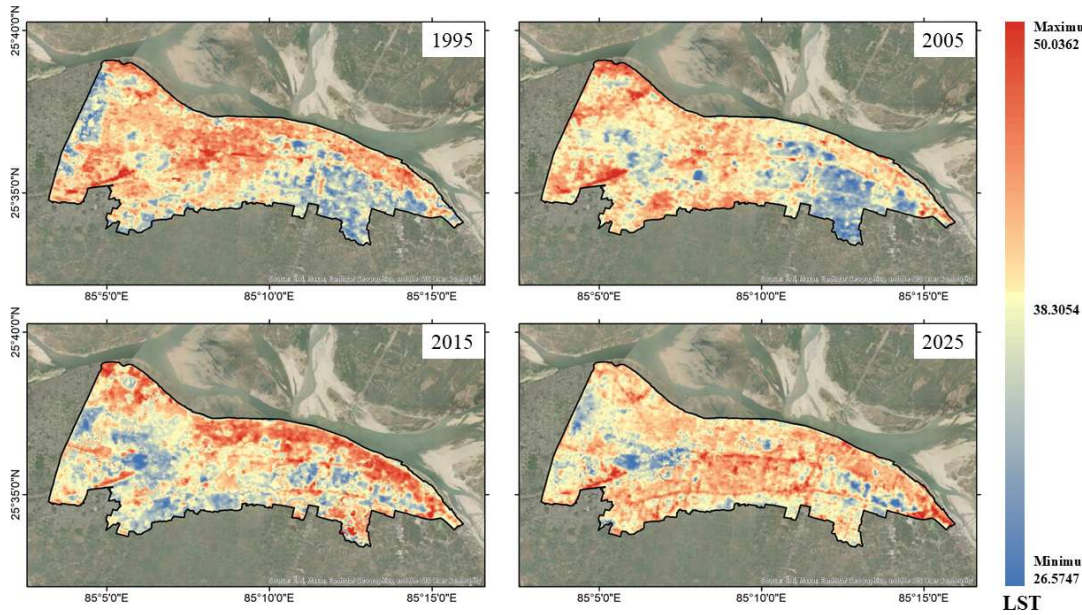


Fig. 4: Spatial distribution maps of LST for the benchmark years 1995, 2005, 2015, and 2025.

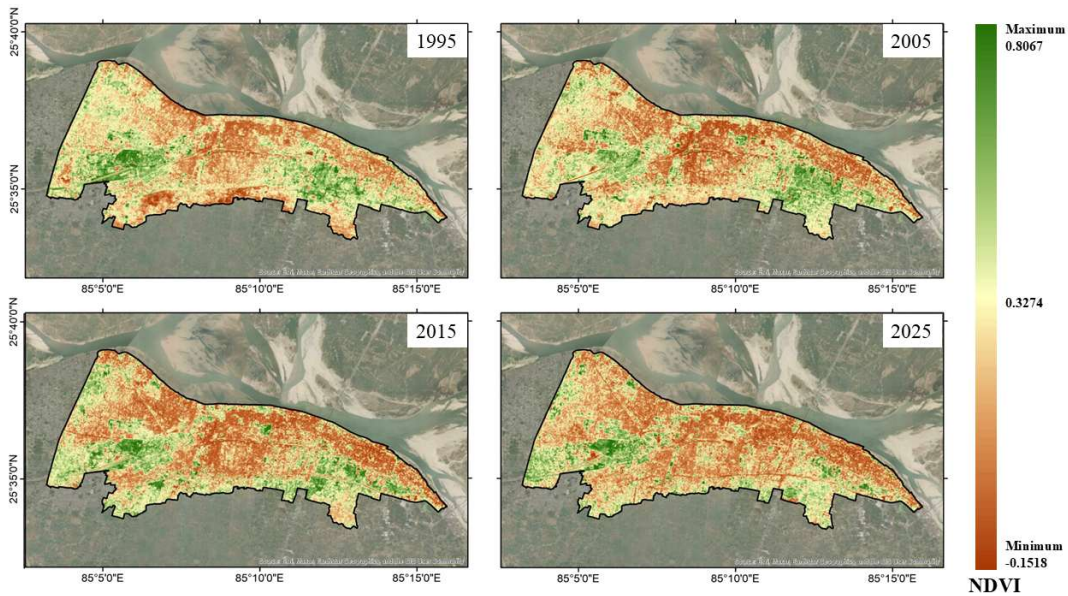


Fig. 5: Spatial distribution maps of NDVI for the benchmark years 1995, 2005, 2015, and 2025.

that while vegetation has not completely disappeared, its spatial arrangement limits its capacity to influence city-scale thermal patterns.

NDBI maps demonstrate the most consistent and unidirectional spatial evolution. In 1995, built-up intensity is moderate and spatially heterogeneous, concentrated mainly in the urban core, with gradual attenuation toward the periphery. Built-up patches are distinct but not spatially dominant, allowing non-built surfaces to retain a significant presence. By 2005, high NDBI values expand substantially, forming more continuous built-up clusters across the central and eastern parts of the city. The spatial contiguity of impervious surfaces increases, and transitional zones between built-up and non-built-up areas become narrower.

In 2015, built-up intensity exhibits near-continuous dominance across much of the urban area. High NDBI zones merge spatially, reducing internal heterogeneity and creating a largely uninterrupted impervious surface network. Peripheral areas that previously showed lower built-up intensity are increasingly absorbed into the urban fabric. By 2025, NDBI maps reveal a highly consolidated built-up structure. High NDBI values dominate almost the entire city extent, with minimal low-intensity zones remaining. The spatial pattern reflects strong urban contiguity and extensive surface sealing, closely mirroring the spatial dominance observed in the LST maps.

The spatial consolidation of high-LST zones observed in the maps is consistent with the statistically significant warming trend identified by the Modified Mann–Kendall analysis ($Z = +2.14$, $p = 0.032$) and the estimated Sen's slope of $+0.1308°C\ yr^{-1}$, indicating a sustained long-term increase in surface temperature across the city.

The spatial evolution of LST, NDVI, and NDBI maps illustrates a progressive shift from a heterogeneous urban landscape to one characterized by built-up continuity, vegetation fragmentation, and thermal homogenization at high temperature levels. The increasing spatial alignment between high NDBI and high LST zones, alongside the fragmentation of NDVI patches, underscores the structural transformation of Patna's surface environment over the last three decades.

3.5. Correlation Analysis Between LST, NDVI and NDBI

Pearson correlation results for the 1995–2025 period are presented in Table 3. A statistically significant positive association is observed between LST and NDBI. Pearson's correlation coefficient is $r = +0.381$ ($p = 0.035$), and Spearman's rank correlation coefficient is $\rho = +0.383$ ($p = 0.033$). The significance in both parametric and nonparametric tests confirms the robustness of the association.

Spearman correlation results for the 1995–2025 period are shown in Table 4. In contrast, the relationship between LST and NDVI is weak and statistically insignificant. Pearson's r is +0.183 ($p = 0.325$), and Spearman's ρ is +0.067 ($p = 0.719$). No significant monotonic or linear relationship is observed.

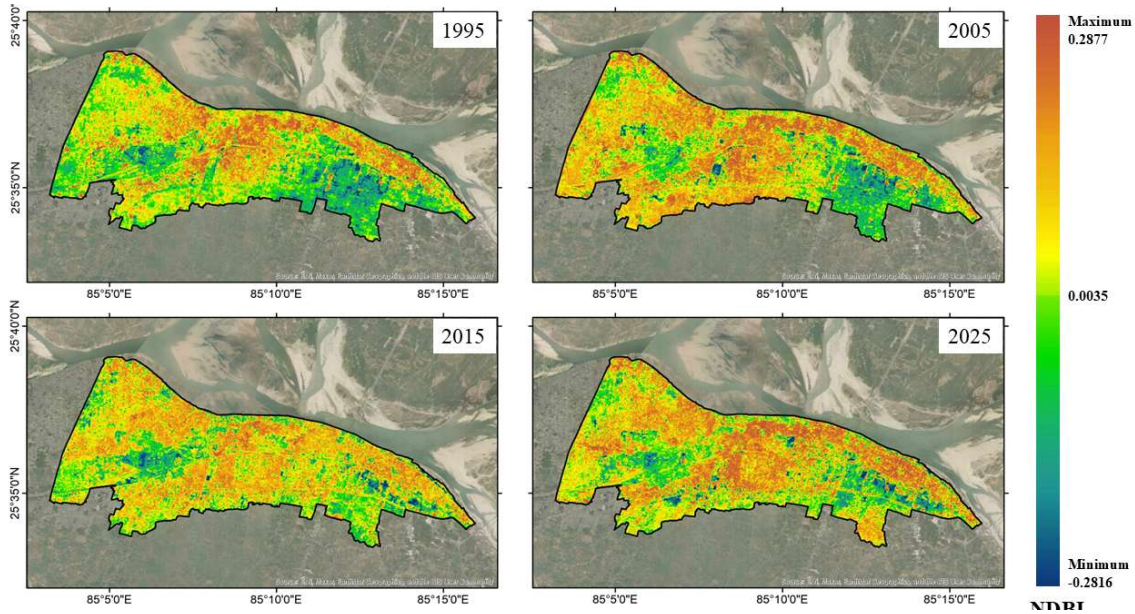


Fig. 6: Spatial distribution maps of NDBI for the benchmark years 1995, 2005, 2015, and 2025.

Table 3: Pearson's correlation results for the 1995–2025 period.

Variable	LST	NDBI	NDVI
LST	1.000	0.381 (p = 0.035)	0.183 (p = 0.325)
NDBI	0.381 (p = 0.035)	1.000	–0.035 (p = 0.852)
NDVI	0.183 (p = 0.325)	–0.035 (p = 0.852)	1.000

Table 4: Spearman's correlation results for the 1995–2025 period.

Variable	LST	NDBI	NDVI
LST	1.000	0.383 (p = 0.033)	0.067 (p = 0.719)
NDBI	0.383 (p = 0.033)	1.000	–0.087 (p = 0.643)
NDVI	0.067 (p = 0.719)	–0.087 (p = 0.643)	1.000

The association between NDVI and NDBI is also weak and statistically insignificant, with Pearson's r = –0.035 (p = 0.852) and Spearman's ρ = –0.087 (p = 0.643).

3.5.1. Hotspot Persistence Metrics

Hotspot persistence metrics derived from LST-class area time series are summarized in Table 5. High-LST zones (Class 4) appear in 100% of years across the study period. The first year of dominance is 2005, after which the Class 4 area remains consistently above ~95% of the total urban area.

The persistence duration of hotspot dominance spans 21 consecutive years (2005–2025). No reversal occurrences are recorded, and area stability is approximately 98%, derived from post-2005 variability. These metrics indicate continuous and uninterrupted persistence of high-temperature zones once dominance is established.

This visual pattern corresponds closely with the quantitative hotspot persistence metrics presented in Table 5, which indicate that high-temperature zones remained dominant for approximately 21 consecutive years (2005–2025) with an estimated spatial stability of about 98%.

3.5.2. Multiple Linear Regression Results

Results of the multiple linear regression analysis are presented in Table 6. Mean LST is modeled as a function of mean NDBI and mean NDVI. The regression model yields an R^2 of 0.183 and an adjusted R^2 of 0.125, with an F-statistic of 3.15 (p = 0.0586). The Durbin–Watson statistic of 2.28 indicates no significant autocorrelation in the residuals.

Mean NDBI exhibits a positive and statistically significant coefficient (β = +27.60, p = 0.031). Mean NDVI shows a positive but statistically insignificant coefficient (β = +14.90, p = 0.261). The intercept term is statistically significant (p < 0.001).

Among the predictors, mean NDBI is the only variable demonstrating statistical significance, while NDVI does not independently explain variation in mean LST within the regression framework.

Table 5: Hotspot persistence metrics derived from LST class area time series.

Metric	Value
First dominance year	2005
Persistence duration	21 years (2005–2025)
Area stability (%)	≈ 98%
Reversal occurrences	0

Table 6: Results of the multiple linear regression analysis.

Predictor	Coefficient (β)	Std. Error	t-value	p-value
Intercept	32.159	4.252	7.56	<0.001
Mean NDBI	+27.602	12.169	2.27	0.031
Mean NDVI	+14.900	12.974	1.15	0.261

4. DISCUSSION

4.1. Interpretation of Long-Term Thermal Dynamics in Patna

The observed warming trend in Patna is consistent with findings from other rapidly urbanizing cities in India, where significant increases in land surface temperature have been linked to rapid urban expansion and impervious surface growth. For example, Mukherjee & Singh (2020) and Kanga et al. (2022) reported similar warming patterns associated with land-use transformation in Ahmedabad and Bengaluru, indicating that sustained urban development can substantially modify local thermal environments.

The statistically significant upward trend in LST, coupled with the exceptionally strong and monotonic increase in built-up intensity, indicates that Patna's thermal trajectory reflects a long-term structural shift rather than short-term climatic fluctuation. The absence of a compensatory long-term trend in vegetation greenness further suggests that the city's natural cooling capacity has not kept pace with rapid urban expansion (Rupapara et al. 2025).

At the city scale, the observed warming trajectory reflects the cumulative effect of infrastructure-led growth, including dense residential development, expansion of

road networks, infilling of open plots, and replacement of permeable surfaces with impervious materials (Kumar & Shukla 2022). Since the early 2000s, Patna has experienced accelerated urban densification driven by population growth, housing demand, and transport-oriented development. The sharp consolidation of high-LST areas around 2004–2005 corresponds temporally with intensified construction activity and infrastructural expansion, indicating a transition from a mixed thermal landscape toward one increasingly dominated by heat-retaining surfaces.

The persistence of high-LST zones across nearly the entire urban area after 2005 indicates that surface warming is no longer spatially localized but has become citywide. This suggests that incremental greening or isolated mitigation measures may be insufficient to substantially alter the prevailing thermal conditions under current development trajectories, highlighting the importance of early-stage land-use planning in rapidly urbanizing tropical cities (Kumar & Shukla 2022).

4.2. Built-Up Expansion as the Dominant Driver of Urban Heat

Among the analyzed variables, built-up intensity exhibits the strongest and most consistent association with LST. The strong monotonic trend in NDBI, its statistically significant correlation with LST, and its significance within the regression model collectively indicate that urban expansion plays a central role in shaping surface warming patterns in Patna. This finding reflects the progressive replacement of low-albedo, moisture-retaining surfaces with concrete, asphalt, and other heat-absorbing materials (Kumar et al. 2025a).

The strong association between built-up intensity and LST observed in this study is consistent with numerous remote sensing studies demonstrating that impervious surface expansion increases surface heat storage and reduces evaporative cooling. Similar relationships between NDBI and LST have been documented in studies conducted in Kolkata (Halder et al. 2025a), Florence and Naples (Guha et al. 2018), and several major Indian metropolitan areas.

In Patna, urban growth has largely occurred through horizontal expansion into peri-urban agricultural land and vertical densification within the city core. The proliferation of paved roads, flyovers, parking areas, and high-density residential blocks has increased surface heat storage capacity while reducing evaporative cooling. The concentration of built-up surfaces along major transport corridors and newly developed residential zones is clearly reflected in the spatial distribution and persistence of high-LST areas (Kumar et al. 2025b).

It should be noted that the regression model explains a limited proportion of the variance in mean LST (R^2 = 0.183), indicating that additional factors beyond vegetation greenness and built-up intensity also influence urban thermal dynamics. Urban surface temperature is affected by a range of variables, including urban morphology (building height, density, and street geometry), anthropogenic heat emissions from transportation and energy use, population density, surface material properties, and atmospheric conditions. These variables were not explicitly incorporated into the present analysis due to the lack of consistent long-term datasets covering the full 1995–2025 period. Consequently, the regression results should be interpreted primarily as an indication of the relative influence of land-cover characteristics derived from satellite imagery rather than as a comprehensive causal model of urban heat dynamics. Future studies integrating urban morphological metrics, socio-economic data, and anthropogenic heat estimates could provide a more complete explanation of the drivers of urban thermal variability.

The regression results further indicate that built-up growth exerts a statistically independent influence on LST at the city scale, even after accounting for vegetation conditions. This suggests that the thermal impact of impervious surfaces outweighs any residual cooling benefits provided by fragmented or sparsely distributed vegetation patches when assessed at an aggregated urban scale.

4.3. Fragmented Vegetation and Loss of Thermal Regulation

Contrary to expectations from classical urban climate theory, vegetation greenness does not exhibit a statistically significant long-term relationship with LST at the aggregated city scale (Cui & Shibata 2024). While NDVI values fluctuate interannually, the absence of a monotonic trend suggests that vegetation change in Patna is characterized primarily by redistribution and fragmentation rather than systematic loss or recovery.

This pattern reflects the nature of greening in Patna, which is largely unplanned and spatially uneven. Small parks, roadside trees, institutional campuses, and floodplain vegetation coexist with expanding built-up areas but lack sufficient spatial continuity to exert a measurable cooling influence at the city scale. Seasonal agricultural activity and monsoon-driven greening contribute to short-term NDVI increases, but these do not translate into sustained thermal regulation. The weak and statistically insignificant relationship between NDVI and LST therefore indicates that existing vegetation, as currently configured, is insufficient in extent, density, or spatial arrangement to counteract the

thermal effects of impervious surface expansion. This finding underscores the limitation of isolated greening initiatives when not integrated into a broader urban ecological framework.

It is important to note that the NDVI–LST relationship examined in this study is based on aggregated city-level annual averages, which may mask localized cooling effects associated with specific vegetation features such as parks, institutional campuses, or riverine green corridors. Vegetation–temperature interactions often operate at finer spatial scales, and pixel-level analyses or spatial regression approaches may reveal stronger localized cooling relationships that are not captured by aggregated statistics. Therefore, the absence of a statistically significant NDVI–LST relationship in the present analysis should be interpreted as reflecting city-scale temporal dynamics rather than implying that vegetation has no local cooling influence. Future research incorporating pixel-based spatial modeling or Local Climate Zone frameworks could provide deeper insight into the spatial heterogeneity of vegetation cooling effects within the urban environment.

4.4. Hotspot Persistence and Thermal Path Dependency

One of the most critical contributions of this study is the identification of persistent urban heat hotspots and the detection of a clear shift toward sustained dominance of high-LST zones around 2005. The transition from a heterogeneous thermal landscape to near-complete dominance of high-temperature areas marks a fundamental change in Patna's urban thermal configuration.

The unidirectional transition from lower to higher LST classes, with no observed reversals during the study period, indicates strong path dependency in the city's thermal evolution. Once high-temperature dominance is established, subsequent land-use changes appear to reinforce rather than offset surface warming. This behavior is consistent with mature urban heat island systems, where accumulated built-up mass, reduced soil moisture, and altered surface–atmosphere interactions contribute to self-reinforcing thermal conditions. From a spatial perspective, the persistence of hotspots suggests that heat is increasingly embedded within the urban fabric. Areas that transitioned into high-LST classes remain in this state over extended periods, highlighting the difficulty of achieving rapid thermal mitigation through retroactive measures alone. This reinforces the importance of proactive thermal planning during early urban development stages rather than reliance on post hoc interventions.

It should be noted that the identification of this transition is based on empirical patterns observed in LST class distributions and hotspot persistence metrics. Formal statistical breakpoint detection or spatial regime-shift analysis was not performed in this study. Future research incorporating advanced temporal breakpoint analysis or spatial statistical methods could further refine the characterization of long-term thermal regime transitions in rapidly urbanizing cities.

4.5. Comparison With Existing Studies

The findings of this study align closely with previous urban climate research conducted in Indian and Global South cities. Studies in Delhi, Kolkata, Mumbai, and Bengaluru have reported significant increases in LST associated with built-up expansion and impervious surface growth, supporting the central role of urbanization in driving surface warming (Gorai et al. 2024, Halder & Kumar 2025, Kanga et al. 2022, Mohammad et al. 2022, Mukherjee & Singh 2020). Similar to Patna, these cities often exhibit strong LST–NDBI relationships and weak or inconsistent LST–NDVI associations at aggregated spatial scales.

Compared with some planned cities that maintain extensive green infrastructure networks, the stronger dominance of high-LST zones observed in Patna may reflect differences in urban morphology, green space availability, and land-use regulation. Studies conducted in cities with larger and more connected green spaces often report stronger NDVI–LST cooling relationships, highlighting the importance of vegetation configuration and spatial continuity in moderating urban thermal environments.

However, the extent and persistence of high-LST dominance observed in Patna appear more pronounced than in some larger metropolitan regions. This may reflect differences in urban morphology, planning controls, and the availability of green infrastructure. Compared with planned cities or those with extensive urban parks and water bodies, Patna's organic growth pattern and limited green space integration may contribute to sustained thermal stress.

Contrasting findings in some studies, where vegetation exhibits a stronger cooling influence, are often associated with cities that have implemented large-scale urban greening programs or retained continuous green belts (Ashok 2021). The absence of such spatially extensive greening in Patna helps explain the weak NDVI–LST relationship observed in this study.

4.6. Policy Implications and Strategic Pathways

From a theoretical perspective, this study contributes to urban heat island research by empirically demonstrating long-term thermal persistence and path-dependent warming in a tropical city context. Traditional UHI frameworks often

conceptualize urban heat as a gradient phenomenon driven by land-cover contrasts between urban and rural areas (Evola et al. 2017). The findings here suggest that beyond certain levels of urbanization, cities may transition into thermal regimes characterized by sustained high surface temperatures and limited short-term variability.

The lack of a significant NDVI-mediated cooling effect challenges simplistic assumptions about vegetation as a universally effective mitigation tool. Instead, the results emphasize the importance of vegetation configuration, continuity, and scale in determining thermal outcomes. This refines existing theory by highlighting that vegetation quantity alone is insufficient and that spatial arrangement and integration into the urban matrix are critical. Also, the combined use of trend analysis, correlation testing, and hotspot persistence mapping provides a comprehensive framework for distinguishing transient thermal variability from long-term persistence, contributing methodological advancement to urban climate research.

For urban planners, engineers, and municipal authorities, the findings offer clear operational insights. The strong association between built-up intensity and surface warming indicates that land-use regulation and construction practices play a central role in shaping urban thermal outcomes. Strategies such as controlling building density, promoting reflective materials, and preserving permeable surfaces are therefore likely to be more effective than isolated greening efforts.

The persistence of hotspots highlights priority zones for targeted intervention, such as retrofitting existing neighborhoods with high-albedo pavements, increasing tree canopy along major corridors, and integrating blue–green infrastructure into redevelopment projects. Importantly, the results suggest that mitigation efforts must be spatially strategic and sufficiently large-scale to influence citywide thermal dynamics. For infrastructure development, incorporating thermal performance criteria into road design, housing layouts, and public spaces could reduce future heat accumulation. The evidence of sustained thermal dominance underscores the need to embed heat mitigation considerations into early planning stages rather than relying solely on corrective measures. At the societal level, persistent urban heat has implications for public health, energy consumption, and social equity. Prolonged exposure to elevated surface temperatures disproportionately affects low-income populations living in dense, poorly ventilated housing with limited access to green spaces. The citywide dominance of high-LST zones suggests that thermal stress is no longer confined to specific neighborhoods but represents a systemic urban risk.

From a policy perspective, the findings support the integration of urban heat metrics into climate adaptation and development policies. Municipal master plans, housing policies, and infrastructure programs should incorporate thermal impact assessments alongside conventional environmental indicators. The identification of a shift toward persistent high-temperature conditions highlights the urgency of preventive action in rapidly urbanizing cities that are approaching similar thresholds. At broader scales, the study contributes evidence relevant to national urban missions and climate resilience frameworks by demonstrating how sustained urban expansion can lead to long-lasting thermal regimes, particularly in tropical contexts.

Patna's long-term surface warming is primarily an outcome of sustained built-up expansion, compounded by fragmented and insufficient vegetation cover. The persistence of high-LST zones and the absence of thermal recovery over the study period indicate that the city has entered a phase of prolonged thermal stress. These findings reinforce the need for integrated, forward-looking urban planning strategies that address thermal risk as a core dimension of sustainable urban development.

5. CONCLUSIONS

This study examined the long-term evolution and spatial persistence of urban thermal conditions in Patna, India, using a 31-year (1995–2025) spatiotemporal remote sensing framework. By integrating land surface temperature with vegetation greenness (NDVI) and built-up intensity (NDBI), the research provides a comprehensive assessment of urban thermal behavior and its underlying drivers in a rapidly urbanizing tropical city. The analytical framework combined trend detection, correlation analysis, spatial hotspot persistence mapping, and multivariate regression, enabling robust characterization of both temporal trajectories and spatial stability of urban heat.

The results reveal a statistically significant and sustained increase in land surface temperature across Patna over the study period, indicating a clear long-term warming trajectory. Built-up expansion exhibits the strongest and most consistent upward trend and shows a significant positive association with LST, highlighting urbanization as the dominant driver of surface warming. In contrast, vegetation greenness does not display a statistically significant long-term trend at the aggregated city scale and does not exert a detectable cooling influence on surface temperature, suggesting that existing vegetation patterns are insufficient to offset the thermal impacts of rapid urban growth. A key contribution of this study lies in identifying spatially

persistent urban heat hotspots and documenting a marked transition toward sustained dominance of high-temperature zones beginning in the mid-2000s. Since approximately 2005, high-LST areas have occupied the majority of the urban extent with minimal interannual variability and no evidence of thermal recovery. This unidirectional shift from lower to higher thermal regimes and the long-term stability of hotspot locations indicate strong path dependency in Patna's thermal evolution, reflecting structurally embedded thermal risk rather than short-term climatic fluctuations.

Methodologically, the study advances urban climate research by demonstrating the value of multi-decadal remote sensing analyses for distinguishing enduring thermal patterns from transient variability. The integrated framework applied here offers a transferable approach for assessing long-term urban heat persistence in data-scarce yet climatically vulnerable cities of the Global South, which remain underrepresented in the urban climate literature. Several limitations should be acknowledged. The analysis relies on satellite-derived land surface temperature, which does not directly represent near-surface air temperature or human thermal exposure. The use of city-averaged indices may mask localized cooling effects associated with specific vegetation configurations or recent greening interventions. In addition, the regression framework does not explicitly incorporate other influential factors such as anthropogenic heat emissions, building morphology, or surface material properties. Residual uncertainties related to sensor differences and atmospheric conditions may also persist despite efforts to ensure temporal consistency.

Future research could address these limitations by incorporating finer-scale analyses using Local Climate Zone classifications, integrating socio-economic and demographic data to assess heat exposure and vulnerability, and combining surface temperature with air temperature and human thermal comfort indicators. Scenario-based modeling of urban growth and greening strategies would further support the evaluation of pathways for mitigating persistent thermal stress in rapidly urbanizing tropical cities. Overall, the findings indicate that Patna is experiencing a prolonged phase of elevated thermal stress driven primarily by sustained built-up expansion and fragmented vegetation patterns that provide limited cooling at the city scale. The persistence of high-temperature zones and the absence of thermal recovery underscore the urgency of integrating heat mitigation into urban planning and climate adaptation strategies. Addressing urban heat as a core dimension of sustainable development will be essential for improving long-term resilience and liveability in tropical megacities.

6. ACKNOWLEDGMENTS

The authors express their gratitude to the National Institute of Technology and different faculty members, who provided their expertise for this research.

7. REFERENCES

Amindin, A., Pouyan, S., Pourghasemi, H.R., Yousefi, S. and Tiefenbacher, J.P., 2021. Spatial and temporal analysis of urban heat island using Landsat satellite images. *Environmental Science and Pollution Research*, 28(30), pp.41439–41450. [DOI]

Amir Siddique, M., Boqing, F. and Dongyun, L., 2023. Modeling the impact and risk assessment of urbanization on urban heat island and thermal comfort level of Beijing City, China (2005–2020). *Sustainability*, 15(7), p.6043. [DOI]

Ashok, A., 2021. Monitoring of dynamic wetland changes using NDVI and NDWI-based Landsat imagery. *Remote Sensing Applications: Society and Environment*, 23, p.100547. [DOI]

Beck, P.S.A., Atzberger, C., Høgda, K.A., Johansen, B. and Skidmore, A.K., 2006. Improved monitoring of vegetation dynamics at very high latitudes: a new method using MODIS NDVI. *Remote Sensing of Environment*, 100(3), pp.321–334. [DOI]

Chen, T., 2022. Temporal dynamics of satellite-derived vegetation pattern and growth in an arid inland river basin, Tibetan Plateau. *Global Ecology and Conservation*, 38, p.e02262. [DOI]

Chow, W.T.L., Akbar, S., Heng, S.L. and Roth, M., 2016. Assessment of measured and perceived microclimates within a tropical urban forest. *Urban Forestry & Urban Greening*, 16, pp.62–75. [DOI]

CITY OF PATNA, 2026. *Patna Municipal Corporation (PMC)*. Retrieved August 14, 2026, from https://www.pmc.bihar.gov.in/about.aspx

Cui, L. and Shibata, S., 2024. Exploring climate-adaptive green-space designs for hot and humid climates: lessons from Japanese dry gardens. *Urban Forestry & Urban Greening*, 93, p.128207. [DOI]

Evola, G., Gagliano, A., Fichera, A., Marletta, L., Martinico, F. and Nocera, F., 2017. UHI effects and strategies to improve outdoor thermal comfort in dense and old neighborhoods. *Energy Procedia*, 134, pp.692–701. [DOI]

Gorai, N., Bandyopadhyay, J., Halder, B., Ahmed, M.F., Molla, A.H. and Lei, T.M.T., 2024. Spatio-temporal variation in landforms and surface urban heat island in riverine megacity. *Sustainability*, 16(8), p.3383. [DOI]

Grimm, N.B., Faeth, S.H., Golubiewski, N.E., Redman, C.L., Wu, J., Bai, X. and Briggs, J.M., 2008. Global change and the ecology of cities. *Science*, 319(5864), pp.756–760. [DOI]

Guha, S., Govil, H., Dey, A. and Gill, N., 2018. Analytical study of land surface temperature with NDVI and NDBI using Landsat 8 OLI and TIRS data in Florence and Naples city, Italy. *European Journal of Remote Sensing*, 51(1), pp.667–678. [DOI]

Gupta, N. and Aithal, B.H., 2022. Effects of rising urban temperatures on the wellbeing of the residents. *International Review for Spatial Planning and Sustainable Development*, 10(4), p.5. [DOI]

Halder, N. and Kumar, D., 2025. Towards reviving vernacular architecture in India: insights into the indigenous building traditions. *Journal of the International Society for the Study of Vernacular Settlements*, 12(5), pp.40–54. [DOI]

Halder, N., Kumar, M., Deepak, A., Abuwaer, N.M., Kanwal, Q., Nurdiawati, A. and Al-Ghamdi, S.G., 2026. Urban greenery and outdoor thermal comfort: cooling indicators, mechanisms, and equity implications. *Environmental Research Communications*. [DOI]

Halder, N., Kumar, M., Deepak, A., Kumar, D., Yasmin, N., Ullah, S. and Al-Ghamdi, S.G., 2025a. Spatiotemporal assessment of urban thermal discomfort in Kolkata, India: insights from cloud-based remote

sensing. IEEE Journal of Selected Topics in Applied Earth Observations and Remote Sensing, pp.1–17. [DOI]

Halder, N., Kumar, M., Deepak, A., Mandal, S.K., Azmeer, A., Mir, B.A., Nurdiawati, A. and Al-Ghamdi, S.G., 2025b. The role of urban greenery in enhancing thermal comfort: systematic review insights. Sustainability, 17(6), p.2545. [DOI]

Halefom, A., He, Y., Nemoto, T., Feng, L., Li, R., Raghavan, V., Jing, G., Song, X. and Duan, Z., 2024. The impact of urbanization-induced land use change on land surface temperature. *Remote Sensing*, 16(23), p.4502. [DOI]

Heaviside, C., Macintyre, H. and Vardoulakis, S., 2017. The urban heat island: implications for health in a changing environment. *Current Environmental Health Reports*, 4(3), pp.296–305. [DOI]

Hsu, A., Sheriff, G., Chakraborty, T. and Manya, D., 2021. Disproportionate exposure to urban heat island intensity across major US cities. *Nature Communications*, 12(1), p.2721. [DOI]

Kanga, S., Meraj, G., Johnson, B.A., Singh, S.K., PV, M.N., Farooq, M., Kumar, P., Marazi, A. and Sahu, N., 2022. Understanding the linkage between urban growth and land surface temperature—a case study of Bangalore City, India. *Remote Sensing*, 14(17), p.4241. [DOI]

Khan, B., Rathore, V.S. and Krishna, A.P., 2021. Identification of Desakota region and urban growth analysis in Patna City, India using remote sensing data and GIS. *Journal of the Indian Society of Remote Sensing*, 49(4), pp.935–945. [DOI]

Kumar, D., Maurya, K.K., Mandal, S.K., Halder, N., Mir, B.A., Nurdiawati, A. and Al-Ghamdi, S.G., 2025a. A whole-life carbon assessment of a single-family house in North India using BIM-LCA integration. Buildings, 15(13), p.2195. [DOI]

Kumar, D., Maurya, K.K., Mandal, S.K., Mir, B.A., Nurdiawati, A. and Al-Ghamdi, S.G., 2025b. Life cycle assessment in the early design phase of buildings: strategies, tools, and future directions. Buildings, 15(10), p.1612. [DOI]

Kumar, D. and Shukla, B., 2022. Urban green spaces for promoting healthy living and wellbeing: prospects for housing. *ECS Transactions*, 107(1), pp.18835–18857. [DOI]

Kumar, S. and Rajak, F., 2023. Assessment of urban green open spaces of micro- and meso-level zones, based on the growth pattern: case of Patna City. *Sustainability*, 15(2), p.1609. [DOI]

Ma, W., Yu, Z., Chen, J., Yang, W., Zhang, Y., Hu, Y., Shao, M., Hu, J., Zhang, Y., Zhang, H. and Yang, G., 2025. What drives the cooling dynamics of urban vegetation via evapotranspiration and shading under extreme heat? *Sustainable Cities and Society*, 130, p.106659. [DOI]

Mahata, B., Sankar Sahu, S., Sardar, A., Laxmikanta, R. and Maity, M., 2024. Spatiotemporal dynamics of land use/land cover (LULC) changes and its impact on land surface temperature: a case study in New Town Kolkata, eastern India. *Regional Sustainability*, 5(2), p.100138. [DOI]

Mishra, A. and Arya, D.S., 2024. Assessment of land-use land-cover dynamics and urban heat island effect of Dehradun city, North India: a remote sensing approach. *Environment, Development and Sustainability*, 26(9), pp.22421–22447. [DOI]

Mishra, M. and Patel, N., 2025. Assessing urban morphology through street parameters in Patna Municipal Corporation, India, through geoinformatics. *Mitteilungen Klosterneuburg*. [DOI]

Mohamed, A., Lorestani, N. and Shabani, F., 2025. Impact of urbanization on land surface temperature: a global perspective. *Current Research in Environmental Sustainability*, 10, p.100315. [DOI]

Mohammad, P., Goswami, A., Chauhan, S. and Nayak, S., 2022. Machine learning algorithm-based prediction of land use land cover and land surface temperature changes to characterize the surface urban heat island phenomena over Ahmedabad city, India. *Urban Climate*, 42, p.101116. [DOI]

Mohan, M. and Kandya, A., 2015. Impact of urbanization and land-use/land-cover change on diurnal temperature range: a case study of tropical urban airshed of India using remote sensing data. *Science of the Total Environment*, 506–507, pp.453–465. [DOI]

Mukherjee, F. and Singh, D., 2020. Assessing land use–land cover change and its impact on land surface temperature using LANDSAT data: a comparison of two urban areas in India. *Earth Systems and Environment*, 4(2), pp.385–407. [DOI]

Nath, R., 2025. Modeling urban thermal dynamics and land use change in Guwahati: a machine learning-based analysis of LST and UTFVI trends (2000–2040). *SSRN Electronic Journal*. [DOI]

Pradeep Kumar, B., Anusha, B.N., Raghu Babu, K. and Padma Sree, P., 2023. Identification of climate change impact and thermal comfort zones in semi-arid regions of AP, India using LST and NDBI techniques. *Journal of Cleaner Production*, 407, p.137175. [DOI]

Priya, U.K. and Senthil, R., 2024. Enhancing sustainable thermal comfort of tropical urban buildings with indoor plants. *Buildings*, 14(8), p.2353. [DOI]

Qi, L., Hu, Y., Bu, R., Li, B., Gao, Y. and Li, C., 2024. Evaluation of the thermal environment based on the urban neighborhood heat/cool island effect. *Land*, 13(7), p.933. [DOI]

Rasul, A., Balzter, H., Smith, C., Remedios, J., Adamu, B., Sobrino, J., Srivanit, M. and Weng, Q., 2017. A review on remote sensing of urban heat and cool islands. *Land*, 6(2), p.38. [DOI]

Sachindra, D.A., Ullah, S., Zaborski, P., Nowosad, M. and Dobek, M., 2023. Temperature and urban heat island effect in Lublin city in Poland under changing climate. *Theoretical and Applied Climatology*, 151(1–2), pp.667–690. [DOI]

Seto, K.C., Güneralp, B. and Hutyra, L.R., 2012. Global forecasts of urban expansion to 2030 and direct impacts on biodiversity and carbon pools. *Proceedings of the National Academy of Sciences*, 109(40), pp.16083–16088. [DOI]

Siddiqui, F.A., Singh, R. and Prashant, 2022. Seasonal characterization and possible solutions for municipal solid waste management in the city of Patna, Bihar, India. *Nature Environment and Pollution Technology*, 21(5), pp.2073–2087. [DOI]

Spangler, K.R., Liang, S. and Wellenius, G.A., 2022. Wet-bulb globe temperature, universal thermal climate index, and other heat metrics for US counties, 2000–2020. *Scientific Data*, 9(1), p.326. [DOI]

Rupapara, S., Rathod, V., Rupapara, H., Halder, N. and Kumar, D., 2025. Evaluating the benefits of urban greenery in urban heat island mitigation: methods, indicators and gaps. *Nature Environment and Pollution Technology*, 24(4), p.D1812. [DOI]

Voogt, J.A. and Oke, T.R., 2003. Thermal remote sensing of urban climates. *Remote Sensing of Environment*, 86(3), pp.370–384. [DOI]

Weng, Q., Lu, D. and Schubring, J., 2004. Estimation of land surface temperature–vegetation abundance relationship for urban heat island studies. *Remote Sensing of Environment*, 89(4), pp.467–483. [DOI]

Zhou, D., Zhao, S., Liu, S., Zhang, L. and Zhu, C., 2014. Surface urban heat island in China's 32 major cities: spatial patterns and drivers. *Remote Sensing of Environment*, 152, pp.51–61. [DOI]